MATCHED FIELD PROCESSING LOCALIZATION WITH RANDOM SENSOR TOPOLOGIES

Joel B. Harley, José M.F. Moura

Carnegie Mellon University
Department of Electrical and Computer Engineering
Pittsburgh, PA 15213

ABSTRACT

One of the largest challenges for multichannel localization systems is developing methodologies that are robust to interference. Unlike noise, interference is not random and often has characteristics resembling the true signals of interest. Interference often originates from multipath propagation, jamming signals, or other sources. In this paper, we demonstrate that we can significantly improve localization performance in the presence of interference through the use of a random sensor topology and matched field processing. To show this, we apply concepts and results from random matrix theory and compressed sensing. We demonstrate theoretically that random sensor topologies allow us to achieve performance characteristics similar to those of random noise. Specifically, we show that the localization performance improves, with a high probability, at a rate proportional to the number of sensors in the system. We verify these results through simulation.

Index Terms— random sensor topology, matched field processing, compressed sensing, random matrix theory

1. INTRODUCTION

Matched field processing is a model-based "generalized beamforming" framework for localizing sources in complex media [1, 2, 3]. Matched field processing is generalized in the sense that sensors do not have to be arranged in a particular configuration and is implemented with a known, arbitrary propagation model of the environment. Matched field processing has been studied and utilized extensively for many applications, including radar [4], underwater acoustics [5], seismology [6], and nondestructive testing [7, 8]. The flexibility of matched field processing also makes it an attractive tool for source localization with sensor networks and cyber-physical systems.

In all of these scenarios, interference presents a significant challenge to developing accurate localization methods. Although effective under random noise, matched field processing and other localization frameworks are often sensitive to unmodeled interference [9]. In many applications, interference may originate from reflective boundaries, other sources in an environment, or signal jamming. Unlike noise, interference is not random and often shares characteristics with the signals of interest, creating significant ambiguity in the measured data.

In this paper, we show that matched field processing can achieve excellent robustness to unmodeled interference when sensors are arranged randomly in space. Several researchers have applied randomly positioned sensor networks and arrays for localization with various methods [10, 11, 12, 13, 14]. We expand on the literature by integrating and analyzing random topologies with coherent matched field processing and analytically determining the performance rates through the use of concepts from compressed sensing [15, 16, 17].

Our results demonstrate that, given the right conditions, the localization performance will improve, with a high probability, at a rate directly proportional to the number of sensors in the system. In comparison, the output signal-to-noise ratio for the coherent matched field processor also improves with a rate directly proportional to the number of sensors in the system. Therefore, the coherent matched field processor, with a random sensor topology, treats interference and random noise in a similar, predictable manner. We validate these results through simulation.

2. PROBLEM FORMULATION

2.1. Signal model

In this section, we present the signal and interference models used in this paper. We assume the signal of interest originates from a single point source and arrives at our sensors as plane waves. Physically, this represents a "far-field" assumption, i.e., the distance between the source and each sensor is greater than two wavelengths λ. We define a measured plane wave signal $x(r,t)$ at a single sensor as

$$x(r,t) \quad = \quad \int_{-\infty}^{\infty} G(\omega)\, e^{-j[k(\omega)r-\omega t]}\, d\omega\,, \qquad (1)$$

where $k(\omega)$ is a function of the wavenumber at each angular frequency ω and $G(\omega)$ is the frequency response of the mea-

This material is based upon work supported by the National Science Foundation Graduate Research Fellowship under Grant No. 0946825.

sured wave. The wavenumber is inversely proportional to the wavelength $\lambda(\omega) = 2\pi/k(\omega)$ of the plane wave. The parameter r represents the distance traveled by the plane wave from its origin to the sensor. If $k(\omega)$ is linear with respect to ω, the wave has a constant group delay across all frequencies. If the $k(\omega)$ is not linear, the plane wave is said to be dispersive and contains a varying phase delay and group delay across the frequency domain.

To measure plane wave signals, we assume we have a collection of M sensors distributed across a space or medium. We also assume the sensors measure each signal at $t = t_0$ and that each signal contains Q discrete frequency components. Therefore, the signal measured at a single sensor is defined by

$$x(r, t_0) = \sum_{q=1}^{Q} V(\omega_q)\, e^{-jk(\omega_q)r} , \tag{2}$$

where $V(\omega_q) = G(\omega_q)e^{j\omega_q t_0}$ and is the complex amplitude of the signal at each frequency ω_q for $1 \leq q \leq Q$. We represent the multichannel signal $\mathbf{x}_s(\mathbf{r}_0)$, corresponding to multiple distances $\mathbf{r}_0 = [r_1\ r_2\ \ldots\ r_N]^T$ between the single source and M different receivers, as an $M \times 1$ vector

$$\mathbf{x}_s(\mathbf{r}_0) = [x(r_1, t_0)\ x(r_2, t_0)\ \ldots\ (r_M, t_0)]^T . \tag{3}$$

We can also represent the multichannel signal vector as a matrix-vector product where

$$\mathbf{x}_s(\mathbf{r}_0) = \boldsymbol{\Phi}(\mathbf{r}_0)\mathbf{v} \tag{4}$$

$$\boldsymbol{\Phi}(\mathbf{r}_0) = \left[e^{-jk(\omega_j)r_i}\right]_{ij} \tag{5}$$

$$\mathbf{v} = [V(\omega_1)\ V(\omega_2)\ \ldots V(\omega_Q)]^T . \tag{6}$$

The $M \times Q$ matrix $\boldsymbol{\Phi}(\mathbf{r})$ represents a plane wave basis where each column represents a unit plane wave signal for the sensors at a single frequency ω_j with wavenumber $k(\omega_j)$. The vector $\mathbf{v}$ contains the complex amplitudes corresponding to each wavenumber in the signal.

For this paper, we assume Q is relatively small such that the measured plane wave is relatively sparse over the frequency domain. We also assume that the wavenumbers of interest and the corresponding $\mathbf{v}$ vector are known. For some applications, the wavenumbers may be estimated from calibration data through the use of sparse recovery methods. This approach has been used in prior work to estimate unknown wavenumbers in multi-modal plane wave data [18].

2.2. Interference model

We assume the interference measured by each sensor is represented by the same frequency amplitude characteristics $\mathbf{v}$ as the signals of interest. The only difference is that we assume the interference corresponds to alternate travel distances that may be random or correspond to a sources outside the region of interest. Therefore, the measured signal $\mathbf{x}$ can be represented as a summation of the signals of interest $\mathbf{x}_s(\mathbf{r}_0)$ and L interfering signals $\mathbf{x}_I(\mathbf{r}_1, \mathbf{r}_2, \ldots, \mathbf{r}_L)$ and can be represented as

$$\mathbf{x} = \mathbf{x}_s(\mathbf{r}_0) + \mathbf{x}_I(\mathbf{r}_1, \mathbf{r}_2, \ldots, \mathbf{r}_L) \tag{7}$$

$$= \boldsymbol{\Phi}(\mathbf{r}_0)\mathbf{v} + \sum_{\ell=1}^{L} \frac{1}{\eta_\ell} \boldsymbol{\Phi}(\mathbf{r}_\ell)\mathbf{v} \tag{8}$$

where $\boldsymbol{\Phi}(\cdot)$ is defined in (4) and $\mathbf{r}_\ell$ represents an $M \times 1$ vector of distances traveled by each interference signal for $1 \leq \ell \leq L$. Each element in $\mathbf{r}_\ell$ is the distance traveled from the interference source to each sensor. The parameter η_ℓ specifies the signal-to-interfere ratio for each interfering signal ℓ. As mentioned previously, the frequency characteristics, described by $\mathbf{v}$, are equivalent for both the signal of interest and the interfering waves.

2.3. Matched field processing

To implement matched field processing, we construct a grid of points within a spatial region of interest. For each point on the grid, which corresponds to a collection of distances $\mathbf{r}$ from that point to each sensor, we construct a signal model $\mathbf{w}(\mathbf{r})$ that predicts what each sensor should measure given a source at that grid location. For this paper, our model $\mathbf{w}(\mathbf{r})$ is represented by a plane wave without interference

$$\mathbf{w}(\mathbf{r}) = \boldsymbol{\Phi}(\mathbf{r})\mathbf{v} , \tag{9}$$

where $\mathbf{v}$ is a known vector and $\mathbf{r}$ corresponds to a point on the grid. In traditional beamforming, $\mathbf{w}(\mathbf{r})$ represents the weights applied to each sensor measurement.

The measured data $\mathbf{x}$ and the model $\mathbf{w}(\mathbf{r})$ are compared through application of a matched field processor. The output of the matched field processor is known as an ambiguity function $b(\mathbf{r})$ and provides a value of "fitness" between the data and model at each point on the grid. The maximum value of the ambiguity function represents the estimated location of a source. In this paper, we use the coherent matched field processor, defined by [3]

$$b(\mathbf{r}) = \left|\mathbf{w}^H(\mathbf{r})\mathbf{x}\right|^2 . \tag{10}$$

This processor is commonly used and assumes the model is correct up to an unknown constant. As shown in (10), the coherent processor outputs the squared inner-product between the data and the model at each point on the grid.

If we substitute $\mathbf{x}$ and $\mathbf{w}(\mathbf{r})$ in (10) with their matrix-vector product representations found in (7) and (9), respectively, the coherent processor can be represented as

$$b(\mathbf{r}) = \left|\mathbf{v}^H\boldsymbol{\Phi}^H(\mathbf{r})\left(\boldsymbol{\Phi}(\mathbf{r}_0) + \sum_{\ell=1}^{L}\frac{1}{\eta_\ell}\boldsymbol{\Phi}(\mathbf{r}_\ell)\right)\mathbf{v}\right|^2 \tag{11}$$

$$= \left|\mathbf{v}^H\boldsymbol{\Phi}^H(\mathbf{r})\boldsymbol{\Phi}(\mathbf{r}_0)\mathbf{v} + \sum_{\ell=1}^{L}\frac{1}{\eta_\ell}\mathbf{v}^H\boldsymbol{\Phi}^H(\mathbf{r})\boldsymbol{\Phi}(\mathbf{r}_\ell)\mathbf{v}\right|^2 .$$

The expression in (11) shows that the ambiguity function is the squared amplitude of the inner-product between the model and the signal of interest plus the inner-product between the model and the interference. In the following section, we analyze this expression for random sensor topologies.

3. RANDOM SENSOR TOPOLOGY PERFORMANCE

We now assume that each sensor, and therefore the distances $\mathbf{r}$ between each sensor and any point on our grid, are randomly distributed. We assume these distances are distributed so that each element in the matrix $\mathbf{\Phi}(\mathbf{r})$ is represented by a Sub-Gaussian distribution [19].

This can be accomplished by choosing the distances in $\mathbf{r}$ to be sufficiently large so that the phase of each element in $\mathbf{\Phi}(\mathbf{r})$ follows a circular uniform distribution. Since the distribution of directional (or circular) random variables converge to a circular uniform distribution as the variance grows large, we can force each phase term to represent a circularly uniform distribution by (I) defining the sensor locations to be random and widely separated in space and (II) defining the grid so that spacing between each grid point is large. We define large or widely separately such that the distances $\mathbf{r}$ are sufficiently larger than a wavelength λ.

If these conditions are met, it is well known that the matrix $\mathbf{\Phi}(\mathbf{r})$ will satisfy the restricted isometry principle (RIP) [20, 21, 22] defined by

$$(1-\delta_s)\|\mathbf{v}\|^2 \leq \|\mathbf{\Phi}(\mathbf{r})\mathbf{v}\|^2 \leq (1+\delta_s)\|\mathbf{v}\|^2 \ , \tag{12}$$

with a small constant $\delta_s \geq 0$ and s non-zero components in $\mathbf{v}$. RIP states that if δ_s is small, then the matrix $\mathbf{\Phi}(\mathbf{r})$ is nearly orthogonal. Note that RIP is normally applied to underdetermined matrices with sparse vectors $\mathbf{v}$, but RIP is equally applicable to any matrix. To represent the expression in the more common underdetermined representation, we could arbitrarily introduce additional columns into $\mathbf{\Phi}(\mathbf{r})$ with corresponding zero elements in $\mathbf{v}$.

3.1. Restricted nullity property

To derive the performance characteristics of our random sensor topology system, we utilize RIP and a property we refer to as the restricted nullity property (RNP), which was first derived in [8]. RNP is an extension of RIP for pairs of matrices. RNP states that if two matrices $\mathbf{\Phi}(\mathbf{r})$ and $\mathbf{\Phi}(\mathbf{r}_0)$ both satisfy RIP with a small δ_s and if the matrix $1/\sqrt{2}\,(\mathbf{\Phi}(\mathbf{r})+\mathbf{\Phi}(\mathbf{r}_0))$ satisfies RIP with a small δ_s, then the matrix pair satisfies [8]

$$-2\delta_s^{'}\|\mathbf{v}\|^2 \leq \mathbf{v}^H\mathbf{\Phi}^H(\mathbf{r}_0)\mathbf{\Phi}(\mathbf{r})\mathbf{v} \leq 2\delta_s^{'}\|\mathbf{v}\|^2 \tag{13}$$

with a small constant $\delta_s^{'}$.

RNP states that if $\delta_s^{'}$ is small, then the columns of the matrices $\mathbf{\Phi}(\mathbf{r}_0)$ and $\mathbf{\Phi}(\mathbf{r})$ are nearly uncorrelated. For our matrices, RNP is generally satisfied if the distances vectors $\mathbf{r}_0$ and $\mathbf{r}$ are sufficiently random and distinct so that the phases of each element in $\mathbf{\Phi}^H(\mathbf{r}_0)\mathbf{\Phi}(\mathbf{r})$ can also be represented by a circular uniform random variable. This condition is satisfied for the same properties described to satisfy RIP.

3.2. Performance characteristics

In this section, we outline two proofs that obtain the performance characteristics of our matched field processing system with a random sensor topology. Parts of these proofs, which we extend in this paper, are discussed in depth in [8].

Theorem 3.1 *If* $\mathbf{x} = \mathbf{\Phi}(\mathbf{r}_0)\mathbf{v} + \sum_{\ell=1}^{L}\eta_\ell^{-1}\mathbf{\Phi}(\mathbf{r}_\ell)\mathbf{v}$ *for a chosen set of possible* $\mathbf{r}$ *vectors and if each* $\mathbf{\Phi}(\cdot)$ *matrix satisfies RIP with constant* δ_s *and each pair of* $\mathbf{\Phi}(\cdot)$ *matrices satisfy RNP with constant* δ_s*, then the ratio between the coherent matched field processor's ambiguity function at the source* $b(\mathbf{r}_0)$ *and at other locations* $b(\mathbf{r})$ *satisfies*

$$\frac{b(\mathbf{r}_0)}{b(\mathbf{r})} \quad \geq \quad \frac{\eta^2}{(1+\eta)^2}\left[\frac{(1-\delta_s)^2}{4\delta_s^2} - \frac{1+\delta_s}{\eta^2}\right] \ , \tag{14}$$

where η *is defined as the total signal-to-interference ratio*

$$\eta \quad = \quad \left(\sum_{\ell=1}^{L}\eta_\ell^{-1}\right)^{-1} . \tag{15}$$

Proof We outline the proof here. The result can be obtained by separately considering $b(\mathbf{r_0})$ and $b(\mathbf{r})$. For each term, we apply RIP to the terms with equivalent matrix product pairs, e.g. $\mathbf{v}^H\mathbf{\Phi}^H(\mathbf{r}_0)\mathbf{\Phi}(\mathbf{r}_0)\mathbf{v}$, and RNP to terms with different matrix product pairs, e.g. $\mathbf{v}^H\mathbf{\Phi}^H(\mathbf{r}_0)\mathbf{\Phi}(\mathbf{r})\mathbf{v}$. In each situation, the appropriate RIP and RNP inequality is applied in order to find a lower bound for $b(\mathbf{r_0})$ and an upper bound for $b(\mathbf{r})$. The ratio of $b(\mathbf{r_0})$ and $b(\mathbf{r})$ and their inequalities are then computed and RIP is applied once more in the numerator of the result. ∎

Theorem 3.2 *With respect to the number of sensors in the system* M*, the ratio between the coherent processor's ambiguity function at the source* $b(\mathbf{r}_0)$ *and at other locations* $b(\mathbf{r})$ *increases at a rate*

$$\frac{b(\mathbf{r}_0)}{b(\mathbf{r})} \quad = \quad \mathcal{O}\left(M\right) \ . \tag{16}$$

Proof *This theorem is derived from combination of Theorem 3.1 and results from [19], which demonstrate that* $\delta_s = \mathcal{O}(1/\sqrt{M})$*. By substituting this expression for* δ_s *into* (14) *and simplifying the result, we get*

$$\begin{aligned}\frac{b(\mathbf{r}_0)}{b(\mathbf{r})} &= \mathcal{O}\left(\frac{\eta^2}{(1+\eta)^2}\left[\frac{(1-M^{-1/2})^2}{4M^{-1}} - \frac{1+M^{-1/2}}{\eta^2}\right]\right)\\ &= \mathcal{O}\left(M - M^{-1/2}\right)\\ &= \mathcal{O}\left(M\right) \ . \end{aligned} \tag{17}$$

∎

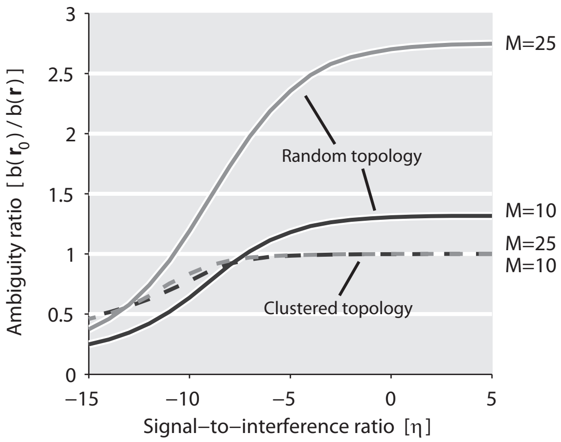

Fig. 1. The average ambiguity ratio of the localization results versus signal-to-interference ratio η for M = 10 (dark lines) and 25 (light lines) sensors. Solid lines show results for a random topology while dotted lines illustrate results for a clustered topology.

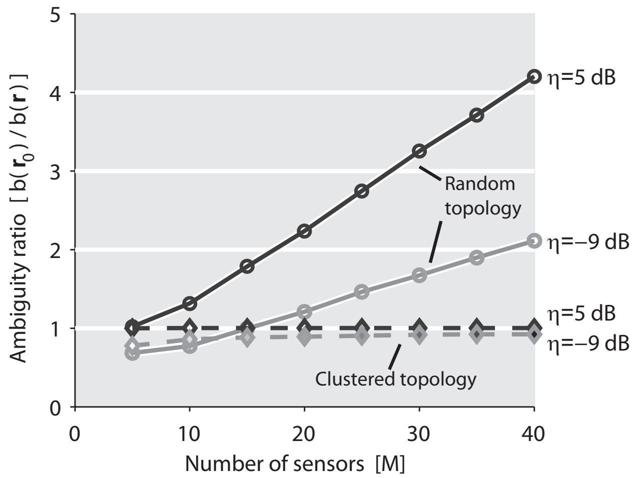

Fig. 2. The average ambiguity ratio of the localization results versus the number of sensors in the system M for signal-to-interference ratios of η = 5 dB (dark lines) and -9 dB (light lines). Solid lines show results for a random topology while dotted lines illustrate results for a clustered topology.

These theorems illustrate the worst-case characteristics for the ambiguity ratio $b(\mathbf{r}_0)/b(\mathbf{r})$. As shown in (14), the ratio increases with respect to the signal-to-interference ratio with a rate of $\mathcal{O}(\alpha(\delta_s) - 1/\eta^2)$ for some constant $\alpha(\delta_s)$. When η is large, the ambiguity ratio is dependent only on δ_s.

Theorem 3.2 and (16) expand on this by showing that the worst-case ambiguity ratio improves with a rate directly proportional to the number of sensors M. This result implies that, if our sensors are distributed randomly in space, we can consistently improve localization by including additional sensors. Since the coherent matched field processor's performance also improves at a linear rate in the presence of random Gaussian noise, our result suggests that the coherent matched field processor, with a random sensor topology, treats interference and noise in a similar predictable manner.

4. SIMULATIONS

We verify the theoretical results through simulation. We consider a 2 m by 2 m two-dimensional region with source located in the area of interest. We assume the source transmits a continuous single-frequency waveform with a wavenumber of $k(\omega) = 500$ cycles/m (a wavelength of approximately 1.25 cm). To perform matched field processing, we choose a grid spacing of 2 cm in the horizontal and vertical directions.

The receiving sensor locations are chosen randomly from independent uniform distributions for the horizontal and vertical directions. We generate interference by assuming that the boundaries of the 2 m by 2 m region act as perfect reflectors and using ray-tracing procedures to determine the distance traveled by each path from the source to each sensor. We simulate every path between the source and each sensor that interacts with a boundary up to five times. We distribute energy equally among each of these interference signals.

We perform a Monte Carlo simulation with 50 different random receiving sensor permutations for a varying number of sensors and varying levels of signal-to-interference ratio. The ambiguity ratio $b(\mathbf{r}_0)/b(\mathbf{r})$ is computed by finding the average ratio between the value at the source and the maximum value within the the remaining grid points.

Figure 1 illustrates the ambiguity ratio as a function of the signal-to-interference ratio and Figure 2 shows the ambiguity ratio as a function of the number of sensors. The solid lines illustrate a random sensor topology that satisfies RIP and RNP with small constants. The dotted lines represent a cluster sensor topology, in which a cluster of sensors are randomly placed in the space, that does not satisfy RIP or RNP with small constants. The sensors are clustered to be positioned within 2 wavelengths of each other. Figure 1 verifies that the ambiguity ratio follows the expression in Theorem 3.1 and Figure 2 verifies that ambiguity ratio improves with a linear rate, as shown in Theorem 3.2.

5. CONCLUSIONS

This paper theoretically demonstrates that we can achieve linear localization performance rates, with respect to number of sensors, when data is corrupted by interference. We show this by integrating the coherent matched field processor, with a random sensor topology, and concepts from compressed sensing and random matrix theory. In future work, we will expand these results in the context of experimental systems.

6. REFERENCES

[1] A.B. Baggeroer, "Matched field processing: Source localization in correlated noise as an optimum parameter estimation problem," *J. Acoust. Soc. Am.*, vol. 83, no. 2, pp. 571, 1988.

[2] A.B. Baggeroer, W.A. Kuperman, and P.N. Mikhalevsky, "An overview of matched field methods in ocean acoustics," *IEEE J. Ocean. Eng.*, vol. 18, no. 4, pp. 401–424, Oct. 1993.

[3] S.E. Dosso and M.J. Wilmut, "Maximum-likelihood and other processors for incoherent and coherent matched-field localization," *J. Acoust. Soc. Am.*, vol. 132, no. 4, pp. 2273–2285, Oct. 2012.

[4] M. Papazoglou and J.L. Krolik, "Matched-field estimation of aircraft altitude from multiple over-the-horizon radar revisits," *IEEE Trans. Signal Process.*, vol. 47, no. 4, pp. 966–976, Apr. 1999.

[5] C. Debever and W.A. Kuperman, "Robust matched-field processing using a coherent broadband white noise constraint processor.," *J. Acoust. Soc. Am.*, vol. 122, no. 4, pp. 1979–1986, Oct. 2007.

[6] D.B. Harris and T. Kvaerna, "Superresolution with seismic arrays using empirical matched field processing," *Geophys. J. Int.*, vol. 182, no. 3, pp. 1455–1477, Sept. 2010.

[7] J.B. Harley and J.M.F. Moura, "Broadband localization in a dispersive medium through sparse wavenumber analysis," in *IEEE International Conference on Acoustics, Speech, and Signal Processing*, Vancouver, BC, May 2013, pp. 4071–4075.

[8] J.B. Harley and J.M.F. Moura, "Data-driven matched field processing for Lamb wave structural health monitoring," *J. Acoust. Soc. Am.*, in preparation.

[9] K. Yang, Y. Ma, and S. Province, "Matched Field Processing in a Mismatch and Multi-source Environment," in *Proc. of MTS/IEEE OCEANS*, Washington, DC, Sept. 2005, pp. 1181–1186.

[10] S.A. Goss, L.A. Frizzell, J.T. Kouzmanoff, J.M. Barich, and J.M. Yang, "Sparse random ultrasound phased array for focal surgery," *IEEE Trans. Ultrason., Ferroelectr., Freq. Control*, vol. 43, no. 6, pp. 1111–1121, Nov. 1996.

[11] R.E. Hudson, C.W. Reed, and F. Lorenzelli, "Blind beamforming on a randomly distributed sensor array system," *IEEE J. Select. Areas Commun.*, vol. 16, no. 8, pp. 1555–1567, Aug. 1998.

[12] X. Sheng and Y. Hu, "Maximum likelihood multiple-source localization using acoustic energy measurements with wireless sensor networks," *IEEE Trans. Sig. Proc.*, vol. 53, no. 1, pp. 44–53, Jan. 2005.

[13] K. Han, Y. Wang, B. Kou, and W. Hong, "Parameters estimation using a random linear array and compressed sensing," *Proc. of International Congress on Image and Signal Processing*, pp. 3950–3954, Oct. 2010.

[14] L. Carin, "Coherence, Compressive Sensing, and Random Sensor Arrays," *IEEE Antennas and Propagation Magazine*, vol. 53, no. 4, pp. 28–39, Aug. 2011.

[15] S.S. Chen, D.L. Donoho, and M.A. Saunders, "Atomic decomposition by basis pursuit," *SIAM J. Sci. Comput.*, vol. 43, no. 1, pp. 129–159, July 1998.

[16] D.L. Donoho, "Compressed sensing," *IEEE Trans. Inf. Theory*, vol. 52, no. 4, pp. 1289–1306, Apr. 2006.

[17] E.J. Candès, J.K. Romberg, and T. Tao, "Stable signal recovery from incomplete and inaccurate measurements," *Comm. Pure Appl. Math.*, vol. 59, no. 8, pp. 1207–1223, Aug. 2006.

[18] J.B. Harley and J.M.F. Moura, "Sparse recovery of the multimodal and dispersive characteristics of Lamb waves," *J. Acoust. Soc. Am.*, vol. 133, no. 5, pp. 2732–2745, May 2013.

[19] R. Vershynin, *Introduction to the Non-Asymptotic Analysis of Random Matrices*, chapter 5, pp. 210–268, Cambridge University Press, Cambridge, 2012.

[20] S. Kunis and H. Rauhut, "Random sampling of sparse trigonometric polynomials, II. orthogonal matching pursuit versus basis pursuit," *Found. Comput. Math.*, vol. 8, no. 6, pp. 737–763, Aug. 2008.

[21] R. Baraniuk, M. Davenport, R. DeVore, and M. Wakin, "A Simple Proof of the Restricted Isometry Property for Random Matrices," *Constr. Approx.*, vol. 28, no. 3, pp. 253–263, Jan. 2008.

[22] H. Rauhut, "Stability results for random sampling of sparse trigonometric polynomials," *IEEE Trans. Inf. Theory*, vol. 54, no. 12, pp. 5661–5670, Dec. 2008.